

Evaluating local properties of magnetic tips utilizing an antiferromagnetic surface

Uwe Kaiser, Alexander Schwarz,* and Roland Wiesendanger
Institute of Applied Physics, Jungiusstrasse 11, D-20355 Hamburg, Germany
 (Received 15 July 2008; published 19 September 2008)

We infer the most relevant local magnetic properties of different iron-coated tips by comparing atomic scale contrasts obtained by magnetic exchange force microscopy utilizing the well-known structural, chemical, and magnetic configurations of NiO(001). Tips with only a single magnetic atom at the apex reflect the genuine antiferromagnetic structure of the nickel atoms, while for magnetic double tips an apparent magnetic contrast on oxygen atoms is observed. Furthermore, we found that even large external flux densities are not sufficient to fully align all magnetic moments of the tip and that local reconfigurations at the apex strongly influence magnitude and direction of the magnetic moments of the foremost tip atom. Knowing what kind of processes take place at tip apices will help to understand and tailor magnetic-sensitive tips for scanning probe techniques.

DOI: 10.1103/PhysRevB.78.104418

PACS number(s): 68.37.-d, 75.25.+z, 75.30.Et, 75.70.-i

It is well known that atomic scale images obtained by near-field scanning probe techniques such as atomic force microscopy (AFM) or scanning tunneling microscopy (STM) contain both sample and tip properties. For instance, an isolated adsorbate will appear twice, if imaged with a structural double tip,¹ and, depending on the kind of the foremost tip atom, a particular kind of atomic species of the surface can be imaged as protrusion or depression.² In the case of magnetic-sensitive techniques such as spin-polarized STM (SP–STM) (Refs. 3 and 4) or the more recently established magnetic exchange force microscopy (MExFM) (Refs. 5 and 6), the problem is even more complex because the image contrast depends also on the magnetic tip properties. Usually one is interested in the sample's properties and assumes that the tip influence is negligible. In this paper we will pursue the inverse approach and image a well-known periodic magnetic structure in order to probe the tip apex using MExFM. For a relatively new technique such as MExFM, which is a promising tool for magnetic imaging with atomic resolution,⁵ it is particularly important to clarify the imaging mechanism as well as possible aberrations due to peculiarities of the used magnetic tips. Their properties are usually quite ill defined and not well controllable. Although we discuss this issue for a particular system, i.e., NiO(001) probed with iron-coated tips, our findings are of general validity and similarly applicable for other tip sample systems or even for SP–STM studies.

For all measurements presented here we employed a home-built force microscope⁷ that uses a flexible cantilever with a sharp tip at its free end as a force sensor. The microscope was operated at 8 K under ultrahigh vacuum conditions utilizing the frequency modulation (FM) technique to probe the tip-sample interaction force (FM–AFM).⁸ In this mode of operation the frequency shift Δf of the cantilever's resonance frequency f_0 is kept constant to record the surface topography, while a second feedback loop keeps the oscillation amplitude A constant. Height variations in constant Δf images on the atomic scale correspond to local variations in the short-range chemical and magnetic exchange forces. Obtaining atomic resolution with FM–AFM in the noncontact (NC) regime (NC–AFM) is well established.⁹ Achieving atomic resolution with MExFM by detecting the short-range magnetic exchange force between the magnetic moments of

the foremost tip atom and the surface atoms was presented by us recently.⁵

The sample in this study used to probe properties of iron-coated tips is NiO(001), which is prepared by *in situ* cleavage and subsequent heating. Chemical, structural, and magnetic properties of this surface are well known: Nickel oxide is an antiferromagnetic insulator with the crystal structure of rocksalt. The surface is nearly bulk terminated (except for a tiny rumpling¹⁰) and exhibits a (1×1) chemical surface unit cell. The magnetic moments of the nickel atoms show a ferromagnetic ordering within (111) planes and an antiferromagnetic one between neighboring (111) planes. Therefore, a row-wise arrangement of the magnetic moments is found at the (001) surface resulting in a (2×1) magnetic surface unit cell. Magnetic ordering is due to superexchange between the nickel atoms mediated by the $2p$ electrons of the bridging oxygen atoms. The magnetic moments of the nickel atoms in the bulk as well as at the (001) surface are canted and point in one of twelve possible $\langle 211 \rangle$ directions.¹¹ For eight of these configurations the polar angle on the (001) surface is about 29.2° , while it is about 60.8° for the other four directions.

From a practical point of view NiO(001) is well suited to evaluate properties of magnetic tips because this system was previously investigated with MExFM (Ref. 5) and density-functional calculations exist for this distinct surface.¹² The tips analyzed in the following were made from silicon and coated *in situ* with about 22 nm of iron. A magnetic-flux density B of 5 T, which is larger than the bulk saturation magnetic polarization of iron ($J_{\text{sat}}=2.1$ T), was applied perpendicular to the sample surface to achieve out-of-plane sensitivity.^{5,6} Note that the antiferromagnetic configuration of NiO(001) will not be altered by 5 T.

Exchange interactions between atomic magnetic moments are mediated by the electron spin and can be described in the Heisenberg model with the Hamiltonian $H = -\sum J_{ij}(\vec{S}_i \cdot \vec{S}_j)$. In this relation, \vec{S}_i and \vec{S}_j are the interacting spins and J_{ij} is the exchange coupling between them. Assuming that only the spins of the foremost tip atom and the underlying surface atom interact during atomic resolution imaging, the magnetic exchange interaction depends strongly on the angle φ between both spins. Maximal and vanishing magnetic interac-

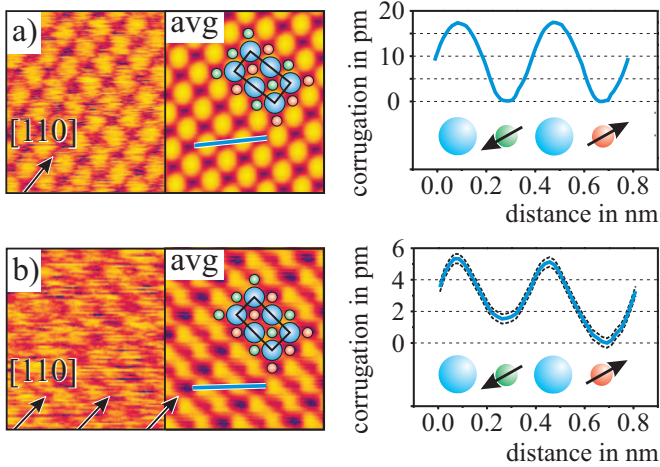


FIG. 1. (Color) (a) AFM and (b) MExFM images of NiO(001), respectively. Both images exhibit the characteristic lattice periodicity. Maxima and minima represent oxygen (blue shaded spheres) and nickel (red and green shaded spheres) atoms, respectively. The MExFM image reveals the row-wise antiferromagnetic arrangement of the nickel atoms and the (2×1) magnetic surface unit cell as reported in Ref. 5. Every second nickel row appears darker than the other ones (see arrows). In the right part of the images averaged representations of the raw data (Ref. 17) are shown. Line sections thereof are presented on the right-hand side. Only in the MExFM data a clear difference between chemically and structurally equivalent rows of nickel atoms is visible, which represents the genuine antiferromagnetic structure of NiO(001) (Ref. 18). Note that the corrugations are different for (a) and (b) since we used different tips and imaging conditions during data acquisition. Parameters: (a) $f_0 = 164\,986$ Hz, $\Delta f = -11$ Hz, $A = \pm 15$ nm, $c_z = 36$ N/m, and $Q_0 = 103\,000$; (b) $f_0 = 158\,995$ Hz, $\Delta f = -23.4$ Hz, $A = \pm 6.7$ nm, $c_z = 34$ N/m, $Q_0 = 27\,700$, and $B = 5$ T.

tion is obtained for (anti)parallel and perpendicular configurations, respectively. To elucidate the influence of the tip on the imaging process in MExFM, we compare experimental results taken with different tips but under similar conditions.

First, the contrast, which corresponds to the genuine configuration of the sample, i.e., NiO(001), has to be identified. Atomic resolution on NiO(001), typically obtained by AFM using a tip without magnetic sensitivity, reveals the (1×1) chemical surface unit cell as shown in Fig. 1(a). The image contrast agrees well with previously published data.^{13–15} In such experiments, an atomically sharp tip is approached to distances of only a few hundred picometers above the surface while the oscillating cantilever is at its lower turnaround point. At these distances the electronic states of the foremost tip atom and the underlying surface atom begin to overlap, resulting in a strong electron-mediated chemical interaction. If a metallic tip is used, the interaction between the tip and sample is expected to be strongest above the oxygen sites because the valence charge density is largest at these positions.¹⁶ Therefore, maxima in constant Δf images of NiO(001) represent oxygen atoms, as indicated by spheres in Fig. 1. In Fig. 1(b) a magnetically sensitive tip is used, resulting in an additional row-wise atomic scale contrast on the minima, i.e., the nickel atoms. This additional modulation on structurally and chemically identical rows of nickel atoms in

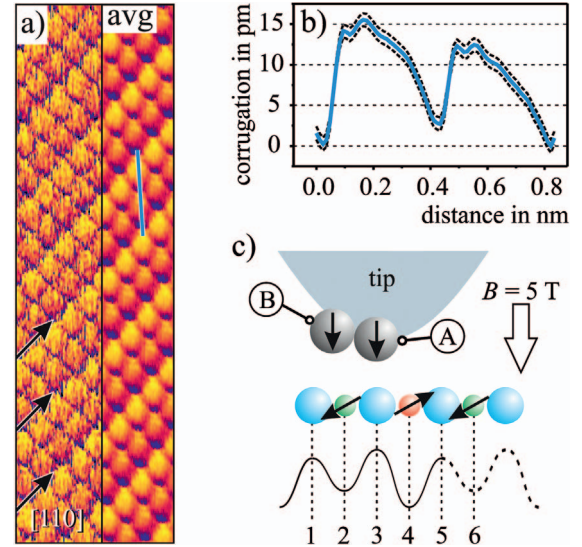


FIG. 2. (Color) (a) MExFM image of NiO(001) recorded with an iron-coated tip showing a magnetic exchange contrast on neighboring rows of nickel atoms and neighboring rows of oxygen atoms [left: raw data; right: averaged data (Ref. 17)]. Darker nickel rows are marked by arrows. (b) Line section obtained from the averaged data. Maxima appear wider than minima and the slopes are asymmetric. (c) Sketch of a magnetic double tip, which can explain the experimentally observed contrast qualitatively (cf. main text). Parameters: $f_0 = 158\,891$ Hz, $\Delta f = -20.5$ Hz, $A = \pm 6.3$ nm, $c_z = 34$ N/m, $Q_0 = 54\,700$, and $B = 5$ T.

MExFM images reflects the genuine antiferromagnetic structure of NiO(001). Since this contrast agrees well with theoretical calculations presented in Ref. 12, where the tip was modeled by a single iron atom, we can infer that Fig. 1(b) represents the contrast expected on NiO(001) if imaged with an iron tip apex for which the foremost tip atom dominates the tip-sample interaction (cf. Ref. 5).

Using Fig. 1(b) as starting point, we can now analyze qualitatively different image contrasts obtained with other tips. For example, in Fig. 2(a) we find a modulation between neighboring rows of nickel atoms and between neighboring rows of oxygen atoms, as clearly visible in the line section in Fig. 2(b). The modulation on neighboring rows of oxygen atoms also has to be of magnetic origin, because, as for the nickel rows, they are structurally and chemically equivalent. However, such a modulation does not reflect the genuine antiferromagnetic structure of NiO(001), which is related to the nickel atoms [cf. Fig. 1(b)]. Hence, the contrast seen in Fig. 2(a) has to be related to the magnetic configuration at the tip apex. It should be mentioned that in Ref. 12 a magnetic moment of $0.07\mu_B$ was determined for surface oxygen atoms. Thus, a small magnetic exchange interaction would also be expected on oxygen atoms. However, the moment for nickel atoms is on the order of $1.16\mu_B$. As visible in the line section in Fig. 2(b), the contrast between oxygen atoms is on the same order of magnitude as on nickel atoms, while the predicted magnetic moments differ by a factor of about 16. Another mechanism to explain the height modulation on the neighboring rows of oxygen atoms would be a superexchange interaction between the foremost tip atom and the

second layer nickel atoms, which are located below surface oxygen rows. If such a mechanism would be also relevant, we would expect to always see a modulation on neighboring rows of oxygen atoms, which is not the case.

The most likely cause, which explains all features observed in Figs. 2(a) and 2(b) qualitatively, is a *magnetic* double tip as sketched in Fig. 2(c). Here, two magnetic atoms (A and B) at the tip apex contribute to the magnetic signal. If the foremost tip atom A is, for example, above the oxygen atom at position 3, the magnetic moment of tip atom B interacts with the magnetic moment at the neighboring nickel site (position 2). As a result, a contrast modulation is found not only on the nickel atoms but on the oxygen sites as well (see the line section). This effect is analogous to a *structural* double tip. However, it should be emphasized again that a pure structural double tip could not result in the observed contrast. The described wedgelike two-atom tip apex model is also strongly supported by the shape of the line section in Fig. 2(b), which reveals maxima that are wider than the minima and asymmetric slopes.¹⁹ In contrast, a single-atom tip apex exhibits symmetric slopes, cf. line section in Fig. 1(b). Note that an iron double tip still allows atomic resolution on NiO(001), because two maxima at this surface (the oxygen atoms) are 417 pm apart, while the iron-iron distance is only about 286 pm (value for bulk α -Fe).

Surprisingly, the magnetic contrast on neighboring rows of oxygen atoms (3.1 ± 0.9 pm) is on the same order of magnitude as on neighboring rows of nickel atoms (2.6 ± 0.9 pm). Intuitively, one would expect that the magnetic contrast on nickel atoms is larger than on oxygen atoms, since the mean tip sample distance above the nickel atoms in this constant Δf image is approximately 12.5 ± 0.9 pm smaller than above the oxygen atoms [cf. Fig. 2(b)]. However, this is possible if the magnetic moment of atom B is farther away but better aligned relative to the canted magnetic moments of the nickel surface atoms than that of atom A (cf. Heisenberg model). This would indicate that 5 T is not sufficient to fully align the magnetic moments at the tip apex along the direction of B .

To achieve a large magnetic signal, the relative orientation between the magnetic moments of the foremost tip atom and the surface atoms is crucial. If antiferromagnetic samples are investigated, an obvious way to control the direction of the magnetic moments of the tip is to apply a sufficiently large external magnetic field that does not alter the sample. However, we found direct proof that even for $B > J_{\text{sat}}$ the magnetic moment at the foremost tip apex atom is not necessarily collinear to B . Figures 3(a) and 3(b) show the same location of the sample imaged by MExFM in 5 T with atomic scale magnetic resolution. The structural defect in the lower left corners, marked by dashed circles, acts as a marker to check the registry of the atomic positions. Between recording images in Figs. 3(a) and 3(b) the tip apex changed its configuration spontaneously. Close inspection reveals a reversal of the magnetic contrast, i.e., rows of nickel atoms with deeper minima in Fig. 3(a) appear as rows of nickel atoms with shallower minima in Fig. 3(b) and vice versa.

How a spontaneous tip change can alter the direction of magnetic moments at the foremost tip atom is explained by employing a simplified two-dimensional tip model sketched

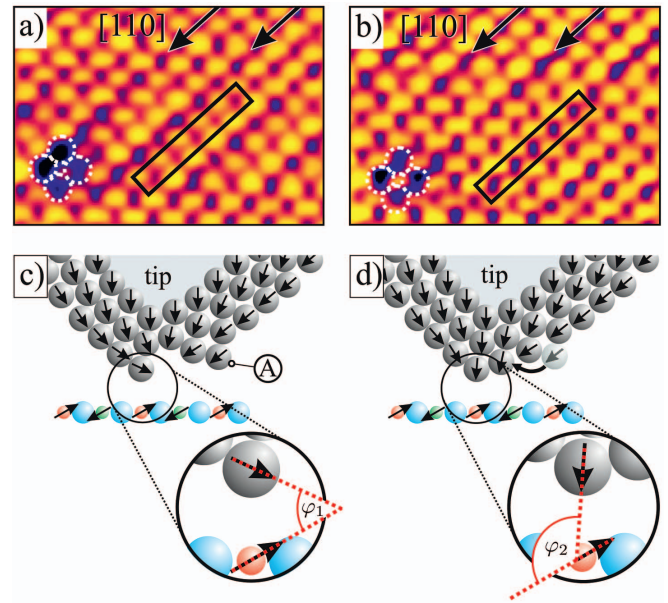


FIG. 3. (Color) MExFM images (low pass filtered) of the same location in NiO(001) recorded before (a) and after (b) a spontaneous tip change. A comparison of identical nickel atoms (e.g., those marked by rectangles) using the defect in the lower left corner as a marker reveals a magnetic contrast reversal. Note that darker nickel rows are marked by arrows. In (c) and (d) a simplified tip model is shown that explains the reversal of the magnetic contrast on NiO(001) with canted magnetic moments. A spontaneous jump of atom A close to the tip apex alters the direction of the magnetic moment at the foremost tip atom via spin-orbit coupling. In the given example the angle between the magnetic moments of tip and sample atom changes from $\varphi_1 \approx 55^\circ$ to $\varphi_2 \approx 125^\circ$. Parameters: $f_0 = 158\,891$ Hz, $\Delta f = -21$ Hz, $A = \pm 6.3$ nm, $c_z = 34$ N/m, $Q_0 = 54\,700$, and $B = 5$ T.

in Figs. 3(c) and 3(d). Let us first list the energy contributions, which govern the direction of the magnetic moments of the tip: The Zeeman energy forces magnetic moments parallel to B . However, even if $B > J_{\text{sat}}$, magnetic moments at the side faces of the tip are rotated into an orientation parallel to the surface of the iron film due to the shape anisotropy, which is in our case perpendicular to B at the tip apex.⁶ Therefore, the magnetic moments at the tip apex are likely to be in a noncollinear frustrated state. Since the local coordination of the foremost tip apex atom, which is certainly not bulk coordinated, strongly influences the direction of the magnetic moment via spin-orbit coupling, structural reconfiguration will also change the direction of the magnetic moment of the foremost tip atom. Note that the Zeeman energy per atom related to 5 T is on the order of 1 meV, whereas the magnetic exchange energy between closely spaced iron atoms is one order of magnitude larger.

Let us assume that the above-mentioned energy contributions lead initially to an angle of $\varphi_1 \approx 55^\circ$ between the magnetic moments of the foremost tip atom and the canted magnetic moment of the nickel atom as sketched in Fig. 3(c). Spontaneous jumps of an atom near the tip apex, as it was described for a nonmagnetic system in Ref. 20, can now significantly change the alignment of the magnetic moment

at the apex. In Fig. 3(d) the result of such a tip change is shown, where a rearrangement of atoms near the apex modifies the effective local anisotropy energy at the foremost tip atom in a way that an angle of $\varphi_1 \approx 125^\circ$ is found. According to the Heisenberg model the strength of the magnetic exchange interaction scales with the cosine of φ . As a result, the tip configuration in Fig. 3(d) would lead to an inverted magnetic contrast in comparison to the one shown in Fig. 3(c).

In summary, our study of different tips on a well-defined surface demonstrates the important role of the atomic and magnetic configurations at the tip apex. While single-atom tips reflect the genuine magnetic structure at the surface, magnetic double tips could result in an apparent magnetic

signal on atoms, which do not possess a magnetic moment. Moreover, we found that the local anisotropy energy at the tip apex can dominate over the Zeeman energy even if $B > J_{\text{sat}}$. Our observations also highlight the interrelation between atomic configuration and the direction of magnetic moments at the tip apex via spin-orbit coupling. For the future development of magnetic sensitive scanning probe techniques such as MExFM and SP–STM, it is important to know how to interpret the magnetic contrast and to identify possible tip effects, particularly on unknown surfaces and surfaces with complex noncollinear magnetic structures.

We gratefully acknowledge financial support provided by the SFB 668.

*aschwarz@physnet.uni-hamburg.de

¹J. P. Pelz and R. H. Koch, Phys. Rev. B **41**, 1212 (1990).

²A. S. Foster, C. Barth, A. L. Shluger, and M. Reichling, Phys. Rev. Lett. **86**, 2373 (2001).

³S. Heinze, M. Bode, A. Kubetzka, O. Pietzsch, X. Nie, S. Blügel, and R. Wiesendanger, Science **288**, 1805 (2000).

⁴M. Bode, Rep. Prog. Phys. **66**, 523 (2003).

⁵U. Kaiser, A. Schwarz, and R. Wiesendanger, Nature (London) **446**, 522 (2007).

⁶A. Schwarz and R. Wiesendanger, Nanotoday **3**, 28 (2008).

⁷M. Liebmann, A. Schwarz, S. M. Langkat, and R. Wiesendanger, Rev. Sci. Instrum. **73**, 3508 (2002).

⁸T. R. Albrecht, P. Grütter, D. Horne, and D. Rugar, J. Appl. Phys. **69**, 668 (1991).

⁹*Noncontact Atomic Force Microscopy*, edited by S. Morita, R. Wiesendanger, and E. Meyer (Springer, Berlin, 2002).

¹⁰T. Okazawa, Y. Yagi, and Y. Kido, Phys. Rev. B **67**, 195406 (2003).

¹¹F. U. Hillebrecht, H. Ohldag, N. B. Weber, C. Bethke, U. Mick, M. Weiss, and J. Bahrtdt, Phys. Rev. Lett. **86**, 3419 (2001).

¹²H. Momida and T. Oguchi, Surf. Sci. **590**, 42 (2005).

¹³H. Hosoi, K. Sueoka, K. Hayakawa, and K. Mukasa, Appl. Surf.

Sci. **157**, 218 (2000).

¹⁴H. Hosoi, K. Sueoka, and K. Mukasa, Nanotechnology **15**, 505 (2004).

¹⁵W. Allers, S. Langkat, and R. Wiesendanger, Appl. Phys. A: Mater. Sci. Process. **72**, S27 (2001).

¹⁶S. Ciraci, A. Baratoff, and I. P. Batra, Phys. Rev. B **41**, 2763 (1990).

¹⁷For periodic lattices all unit cells in the raw data can be used to create a single averaged unit cell with increased signal-to-noise ratio. For a better visualization of the periodicity we tiled a new image together from this averaged unit cell. In line sections taken from averaged images dashed lines indicate the upper and lower bounds of the standard deviation after the averaging procedure.

¹⁸How we can exclude an oscillatory noise as an artificial origin for the modulation is described in the SI of Ref. 5.

¹⁹We can exclude an artifact due to a slow z -feedback regulation, because the asymmetric slopes are found independent of the scan direction.

²⁰R. Hoffmann, A. Baratoff, H. J. Hug, H. R. Hidber, H. v. Löhnneysen, and H.-J. Güntherodt, Nanotechnology **18**, 395503 (2007).